View metadata, citation and similar papers at core.ac.uk
brought to you by CORE
provided by Elsevier - Publisher Connector

Chemistry & Biology
Article

Targeting the Proangiogenic VEGF-VEGFR Protein-Protein Interface with Drug-like Compounds by In Silico and In Vitro Screening

Benoit Gautier,[1,8,9] Maria A. Miteva,[2,8,9] Victor Goncalves,[1] Florent Huguenot,[3,8] Pascale Coric,[4] Serge Bouaziz,[4] Bili Seijo,[4] Jean-François Gaucher,[4] Isabelle Broutin,[4] Christiane Garbay,[1,8] Aurelien Lesnard,[3] Sylvain Rault,[5] Nicolas Inguimbert,[6,8] Bruno O. Villoutreix,[2,8,*] and Michel Vidal[3,7,8,*]
[1]Université Paris Descartes, CNRS UMR 8601, UFR biomédicale, 75006 Paris, France
[2]INSERM U973, Université Paris Diderot, 75013 Paris, France
[3]Université Paris Descartes, CNRS UMR 8638
[4]Université Paris Descartes, CNRS UMR 8015
UFR des Sciences Pharmaceutiques et Biologiques, 75006 Paris, France
[5]CERMN, Centre d'Etudes et de Recherche sur le Médicament de Normandie, 14032 Caen Cedex, France
[6]Université de Perpignan Via Domitia, laboratoire de chimie des biomolécules, 66860 Perpignan, France
[7]Laboratoire de Pharmacologie-Toxicologie, Service de Pharmacie, Hopital Cochin, 75014 Paris, France
[8]INSERM U648, Laboratoire de Pharmacochimie Moléculaire et Cellulaire, 75006 Paris, France
[9]These authors contributed equally to this work
*Correspondence: bruno.villoutreix@inserm.fr (B.O.V.), michel.vidal@parisdescartes.fr (M.V.)
DOI 10.1016/j.chembiol.2011.10.016

SUMMARY

Protein-protein interactions play a central role in medicine, and their modulation with small organic compounds remains an enormous challenge. Because it has been noted that the macromolecular complexes modulated to date have a relatively pronounced binding cavity at the interface, we decided to perform screening experiments over the vascular endothelial growth factor receptor (VEGFR), a validated target for antiangiogenic treatments with a very flat interface. We focused the study on the VEGFR-1 D2 domain, and 20 active compounds were identified. These small compounds contained a (3-carboxy-2-ureido)thiophen unit and had IC_{50} values in the low micromolar range. The most potent compound inhibited the VEGF-induced VEGFR-1 transduction pathways. Our findings suggest that our best hit may be a promising scaffold to probe this macromolecular complex and for the development of treatments of VEGFR-1-dependent diseases.

INTRODUCTION

Protein-protein interactions (PPIs) are pervasive in biology but are classically challenging targets. The human interactome is predicted to include about 650,000 interactions (Stumpf et al., 2008), among which a sizeable number could be modulated by low molecular weight compounds (Wells and McClendon, 2007). Several conceptual and technical hurdles to the efficient targeting of PPIs have been proposed, including the nature of the chemicals present in the compound collections, the plasticity of the interfaces, and access to a relevant in vitro assay (Sperandio et al., 2010b). Furthermore, interfaces are usually large (an average interface area of 1,000–2,000 $Å^2$ is often observed for heterodimeric protein-protein complexes) and flat and have generally not evolved to bind low molecular weight molecules (Higueruelo et al., 2009). Recent successes in the field pave the way for a paradigm shift in drug discovery and basic research (Fry, 2008; Villoutreix et al., 2008; Wells and McClendon, 2007), although it has been pointed out that the macromolecular complexes modulated to date essentially lie toward the more druggable end of the PPI difficulty spectrum (Arkin and Whitty, 2009). One would expect that a protein complex easier to screen most likely has a relatively pronounced cavity at the interface, facilitating the binding of a small molecule. Indeed, the planarity (root-mean-square deviation of all the interface atoms from the least square plane through the atoms) values of most protein-protein complexes successfully inhibited by small molecules tend to be between 2.3 and 3.6 Å (the smaller is the planarity index; the flatter is the surface) (Reynolds et al., 2009), indicating the presence of a relatively deep binding groove (Figure S1 available online). Yet, some very flat interfaces inhibited by a small drug-like molecule have been reported, like, for instance, for the X-linked inhibitor of apoptosis (XIAP), which has a planarity value of 1.8 Å (Arkin and Whitty, 2009; Fry, 2008).

We, thus, decided to revisit several therapeutically important protein-protein interfaces with known three-dimensional (3D) structures. We found that the vascular endothelial growth factor receptor (VEGFR), a protein that binds to the vascular endothelial growth factor (VEGF), had a planarity value of 1.7 Å, well below those of most transient protein-protein complexes (mean planarity value = 2.7 Å; Reynolds et al., 2009). In addition, VEGFR plays a key role in angiogenesis, one of the hallmarks of cancer (Ferrara and Kerbel, 2005; Hanahan and Weinberg, 2000; Hicklin and Ellis, 2005). VEGF binds to two major tyrosine kinase receptors (TKRs), VEGFR-1 and VEGFR-2, on the surface of endothelial cells, thereby activating signal transduction and regulating both physiological and pathological angiogenesis. Whereas VEGFR-1 has been shown to stimulate endothelial cell migration

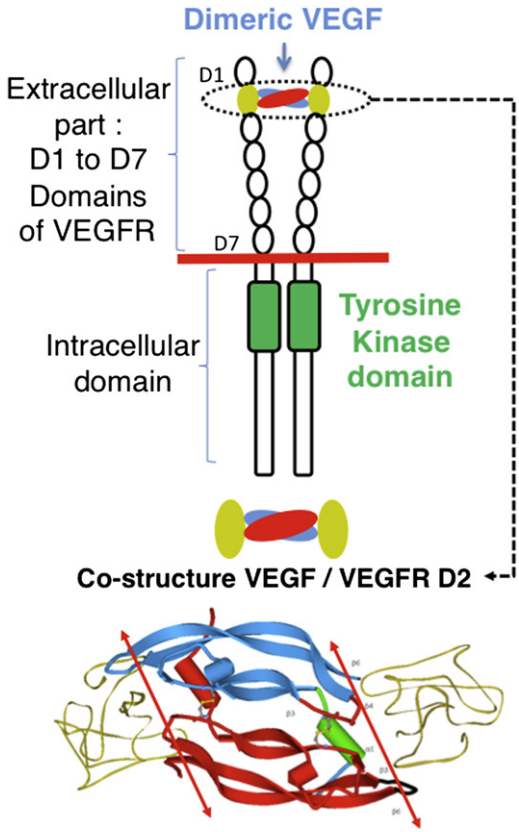

Figure 1. The VEGF-VEGFR-1 Complex
Schematic diagram illustrating our approach for blocking VEGF signaling by inhibition of VEGF-VEGFR PPI. The approach followed in this work does not intend to inhibit the tyrosine kinase site but aims at the inhibition of a PPI (red arrows) through design of a ligand binding to the D2 domain by combining in silico-in vitro screening experiments. See also Figure S1.

(Kanno et al., 2000; Ziche et al., 1997), VEGFR-2 is known to be the main mediator of signaling pathway in endothelial cells (Holmes et al., 2007; Olsson et al., 2006).

Both VEGFR molecules have an extracellular component containing seven immunoglobulin-like domains (extracellular domains [ECDs], D1–D7), a single transmembrane segment, and an intracellular domain with a consensus tyrosine kinase sequence (Shibuya et al., 1990; Terman et al., 1991) (Figure 1). The VEGF-VEGFR interaction or the catalytic activity of the VEGFR is currently targeted by drugs such as bevacizumab (antibody), sunitinib, and sorafenib (tyrosine kinase inhibitors), whereas the soluble receptor (aflibercept) is currently in clinical trials (Grothey and Galanis, 2009; Ivy et al., 2009; Jänne et al., 2009). These drugs are, thus, either injected proteins such as bevacizumab (Avastin) targeting VEGF itself and are not orally active or oral tyrosine kinase inhibitors but are not specific for VEGFR. A small molecule orally available inhibiting the VEGF-VEGFR interaction could, therefore, be of interest as compared to therapeutic proteins because the cost of the treatment should be significantly lower and more convenient to the patient and medical team. The concept has in fact been validated using small peptides (D'Andrea et al., 2005; Gautier et al., 2010; Goncalves et al., 2007a; Jia et al., 2001; Zilberberg et al., 2003) and nondrug-like organic molecules (Ueda et al., 2004a, 2004b), supporting further the rationale of our study.

The overall process to investigate the VEGF-VEGFR complex is illustrated in Figures 1 and 2. We analyzed the surface of the receptor and used structure-based virtual ligand screening (SB-VLS) (Sperandio et al., 2006) to identify drug-like competitive antagonists of the VEGF-VEGFR-1 complex. We identified one series of chemicals able to inhibit the flat VEGF-VEGFR-1 interaction and, subsequently, focused our attention on the most potent compound of this series, molecule **4321** (Table S1). This compound was investigated by NMR and in cellular assays and was found to inhibit the $VEGF_{165}$ (a 165 amino acid isoform of VEGF)-induced VEGFR-1 phosphorylation and endothelial cell tubulogenesis, highlighting its role as a new promising antiangiogenic agent. In addition this molecule was not found to be toxic in WST-1 cell proliferation assays, consistent with its in silico absorption, distribution, metabolism, excretion, and toxicity (ADMET) profile (Table S2).

RESULTS AND DISCUSSION

Binding Pocket Prediction and In Silico Screening

We investigated the crystal structure of the VEGFR-1 D2 domain and carried out a theoretical prediction of possible druggable pockets within and around the experimental protein-protein binding zone. Not only part of the region interacting with VEGF but also subpockets some distance away from this interfacial area were predicted as potentially interesting for docking experiments. However, the surface topology around the binding site of the VEGF on the VEGFR-1 is flat and large (>800 A^2), suggesting that SB-VLS computations could be challenging. We identified three interesting small subpockets with the Surflex-Protomol probe-mapping algorithm (CH4, C = O, and N-H groups were used to search for areas capable of interacting favorably with an incoming ligand) (Jain, 2003) and through interactive structural analysis (Figure 2). We also took into account the results of previously reported mutagenesis studies, which showed that the K16, F17, M18, Y21, Q22, and Y25 amino acid residues of the VEGF N-terminal α helix were potentially important for interactions with VEGFR (Fuh et al., 2006; Keyt et al., 1996; Li et al., 2000; Muller et al., 1997; Pan et al., 2002). Our analysis highlighted a polar subpocket A, formed by residues K170, T206, E208, and K217, a region in contact with the VEGF residue Q22. Subpocket A overlaps only partially with the direct protein-protein interface, but it forms a small crevice within which a small compound could be anchored in this otherwise flat region. Subpocket B consists essentially of hydrophobic/aromatic residues (e.g., of residues Y139, I142, P143, N219, L221) and is in contact with F17 and M18 of the VEGF N-terminal α helix. Two tyrosine groups, Y21 and Y25 of the VEGF α helix, interact with the essentially hydrophobic and planar subpocket C (e.g., of residues Y199, K171, F172, P173, L204). We investigated the overall nature of this region further by identifying key interaction sites with another probe-mapping method (probes = positively charged sp3 nitrogen, a negatively charged sp2 oxygen, and a sp3 carbon) as implemented in LigBuilder (Wang et al., 2000), in which only the strongest interacting groups survive at the surface. Only seven carbon probes remained, mostly located in subpockets B and C, further highlighting the

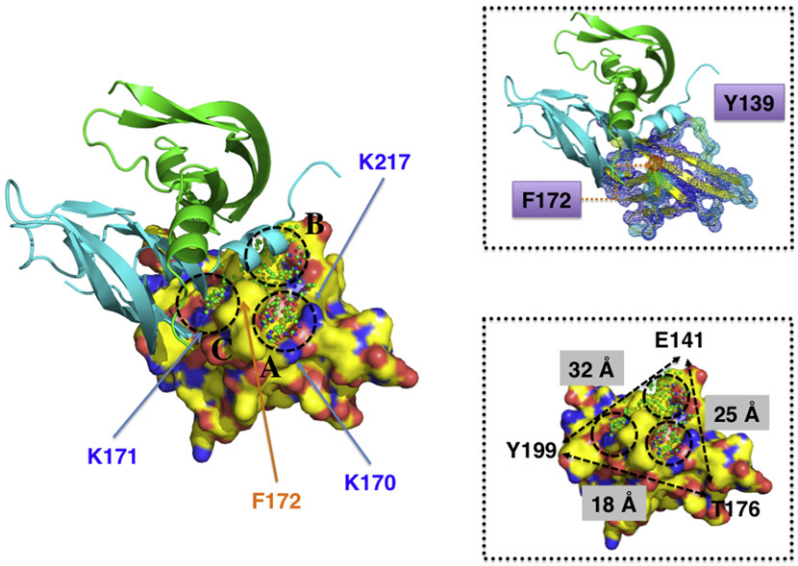

Figure 2. Structural Analysis of the VEGF-VEGFR-1 Complex

Left view shows the crystal structure (Wiesmann et al., 1997) of residues 8–109 of VEGF (VEGF8–109 cartoon diagram) in complex with VEGFR-1 D2 domain (shown here in solid-surface representation: yellow, hydrophobic/aromatic; red, oxygen atom and/or negatively charged; blue, nitrogen atom and/or positively charged). A probe-mapping algorithm (Jain, 2003) was used to analyze the interface area (green sphere highlights regions where carbon atoms can bind with reasonable affinity, blue spheres represent nitrogen atoms, and red spheres, carbonyl groups). Three subpockets, A, B, and C, could be identified and are shown as dashed circles.

Right-top dashed square illustrates the deformability in the screening region that was assessed with the DFprot server (Garzon et al., 2007). Color-coded deformation values are projected on a mesh representation of the receptor. In the screening region, areas of Y139 and F172 are expected to be flexible (deformable regions are in red; regions somewhat more flexible are in light blue and green), whereas the interface itself, color coded in dark blue, appears relatively rigid.

Right-bottom dashed square shows the overall search zone investigated during the docking computations that is delineated by the dashed lines and forms a relatively large triangle.

See also Figure S2.

overall hydrophobic nature of this region. Receptor flexibility is known to be important in some biological systems, and normal mode analysis (NMA) is an efficient method for investigating this property (Cavasotto et al., 2005; Sperandio et al., 2010a). We, thus, carried out NMA on our biological target using the DFprot server, a structural bioinformatic tool that predicts protein deformability starting from a single-input 3D structure (Garzón et al., 2007). Areas of VEGFR-1 residues Y139 and F172 were predicted to be slightly flexible, whereas the direct interface with VEGF appeared rigid (Figure 2). The computed deformability is consistent with the B factors of the crystal structure of VEGFR-1 and with the NMR structures of VEGFR-1 (Starovasnik et al., 1999). These results suggest that it is acceptable to maintain the target rigid during the docking computations assuming that the algorithm is not too sensitive to tight atomic contacts and that the redocking of some compounds would benefit from the use of a method capable of handling the flexibility of some amino acid side chains.

The 8,000 chemical compounds of the Centre d'Etudes et de Recherche sur le Médicament de Normandie (CERMN) library were then docked with Surflex onto the defined target zones, and the predicted binding affinities were initially estimated for each pose with the default scoring function. Because a few residues in this region are predicted to be flexible, we thought that it would be appropriate to take flexibility into account implicitly by tuning the "penetration" parameter of Surflex (please refer to "In Silico Procedures" in the Supplemental Experimental Procedures). The docked compounds were reranked during a post-processing step, with a pocket-tuned scoring function (Miteva et al., 2005a). We selected an initial list of 350 molecules after a visual inspection of the top-ranked 2,500 compounds. These molecules were then analyzed with our rule-based ADMET-filtering package (Lagorce et al., 2008, 2011) and by medicinal chemists. This process led to the selection of a final list of 206 compounds for experimental testing.

Predicted Modes of Binding for the Best Inhibitor

To investigate the likely binding mode of our best inhibitor, compound **4321** (see below), we analyzed different binding poses in the three predicted subpockets A, B, and C (Figure S2). Although the targeted zone is mostly hydrophobic, three or four hydrogen bonds could potentially form between the VEGFR-1 D2 domain and compound **4321**. Additional analyses were then carried out with AutoDock4 (Morris et al., 2009) but this time by allowing explicit flexibility of several amino acid side chains. We found that compound **4321** is most likely binding to subpockets B and C (the three lowest energy positions).

In Vitro VEGF Displacement Assays and the Inhibitors Identified

We assessed the binding of the 206 selected small compounds to VEGFR-1 by a chemiluminescence assay based on competition with biotinylated $VEGF_{165}$ ($btVEGF_{165}$) for binding to the ECDs of VEGFR-1 (VEGFR-1 D1–D7) (Goncalves et al., 2007b) (please refer to "Biological Reagents" in the Supplemental Experimental Procedures). Given the challenging topology of the interface, we initially tested the compounds at a relatively high concentration of 200 μM, at which 33 compounds displayed 21%–100% inhibition. Of these compounds, 6 gave 41%–60% inhibition, 16 gave 61%–80% inhibition, and 11 gave 81%–100% inhibition. We considered molecules giving more than 60% inhibition at 200 μM to be most promising. This criterion identified 20 hits from 1 chemical family (the (3-carboxy-2-ureido)thiophen series; Figure 3; Table S1). These 20 molecules inhibited the formation of the $VEGF_{165}$-VEGFR-1 complex with IC_{50} values of 135–18 μM (Table S1) and appeared to be interesting from a structural, pharmacokinetic, and toxicological standpoint (Table S2).

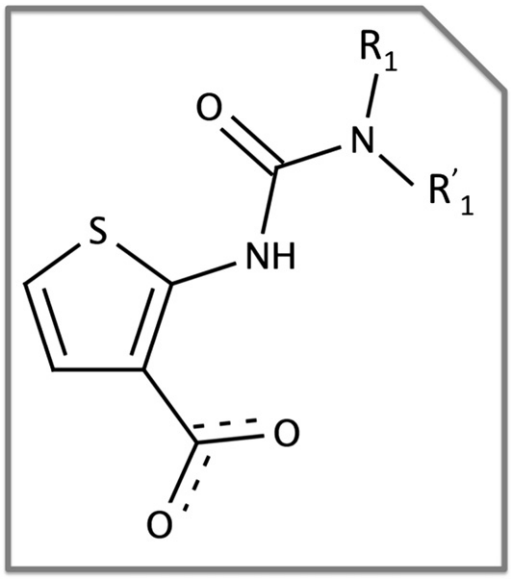

Figure 3. General Structure of the (3-Carboxy-2-Ureido)Thiophen Series

In Compound **4321**: R1, Ethyl; R1′, Benzyl. See also Figure S3, and Tables S1 and S2.

One compound, molecule **4321**, competed with btVEGF$_{165}$ for binding to the ECDs of VEGFR-1 (D1–D7, noted VEGFR-1 ECD) with an IC$_{50}$ value of 18 μM. Ruch et al. (2007) recently showed that VEGF binding to VEGFR-2 induced conformational changes of the receptors, leading to receptor dimerization and intracellular tyrosine kinase activation. These changes result from homotypic interactions between the immunoglobulin-like domains 4 (Barleon et al., 1997) and 7 of the monomers (Ruch et al., 2007). These data suggest that compounds targeting the D4 or D7 domains may act as VEGFR-1 antagonists, preventing dimerization. To rule out this mechanism, we assessed the ability of our compounds to displace the interaction between the VEGFR-1 D1–D3 domains and VEGF. Here, compound **4321** had an IC$_{50}$ value of 10 μM, giving a ligand efficiency of about 0.32 kcal mol^{-1} per nonhydrogen atom (the maximum possible value is about 1.5 kcal mol^{-1}), equivalent to those of many kinase and protease inhibitors (Wells and McClendon, 2007). The resulting displacement curves of both tests are available in Figure S3.

WaterLOGSY Experiments

Several NMR experiments have been designed to characterize the interaction between a ligand and its target protein, such as saturation transfer difference (Mayer and Meyer, 1999), reverse NOE pumping (Chen and Shapiro, 2000), transferred NOE (Meyer et al., 1997), and more recently, the Water-Ligand Observed via Gradient SpectroscopY (WaterLOGSY) experiments (Dalvit et al., 2001). The WaterLOGSY seems to have the higher sensitivity compared to other methods, and we applied this approach to demonstrate that compound **4321** binds to VEGFR-1 D2 and not to VEGF. With this approach it is possible to discriminate between binding and nonbinding ligands according their signal on the NMR spectra.

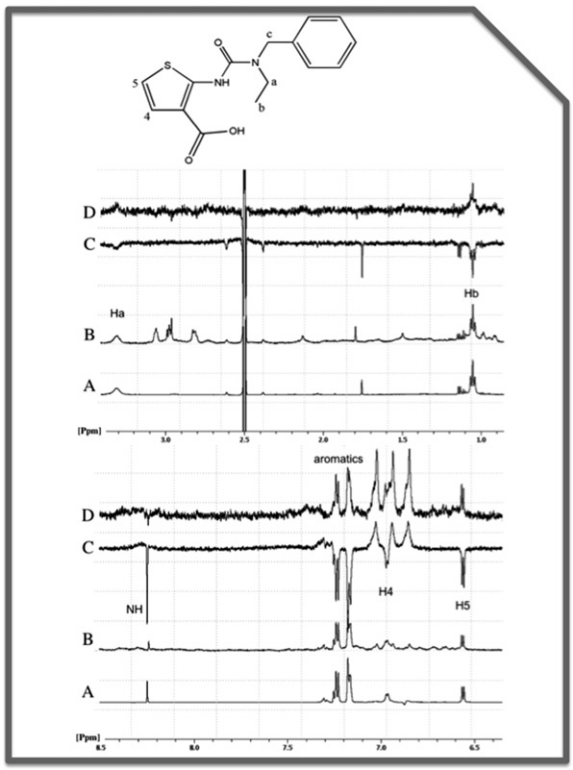

Figure 4. WaterLOGSY Experiments

Structure of the compound **4321**, 1D spectra, and WaterLOGSY spectra of the compound in the absence of the VEGFR-1 D2 (A and C) and in the presence of the domain VEGFR-1 D2 (B and D). The positive signal of the compound on spectra D demonstrates an interaction between the small molecule and the VEGFR-1 D2. Some peaks arising from VEGFR-1 D2 are visible, in particular in the 1D spectra (B) around 3 ppm.

Figure 4 shows the 1D spectra and the WaterLOGSY of the compound **4321** in the absence of the VEGFR-1 D2 (Figures 4A and 4C) and in the presence of the protein (Figures 4B and 4D). The WaterLOGSY of the free compound (Figure 4C) contains several peaks of different intensity with different signals. Protons from molecule **4321** are easily identified, and three extra-broad resonances arising from a quaternary ammonium are observed around 7 ppm. These three last peaks arise from an exchange with water, they are not observed on the basic 1D spectra, and they give a signal of opposite sign in the WaterLOGSY. In the presence of the protein VEGFR-1 D2 (Figure 4C), an inversion of the sign of the resonances from **4321** occurs. The inversion of the signal of **4321** in the WaterLOGSY spectra in presence of the protein is characteristic of its interaction with the protein because as the ligand adopts the tumbling correlation time of the protein, its signal is inverted on the spectra because of the negative NOE.

Compound 4321 Specifically Inhibits the VEGF$_{165}$-Dependent Phosphorylation of VEGFR-1

We analyzed both the biochemical effect and the specificity of compound **4321** by assessing its ability to inhibit the VEGF$_{165}$-induced autophosphorylation of VEGFR-1 and VEGFR-2 (please refer to "Biological Results" in the Supplemental Experimental

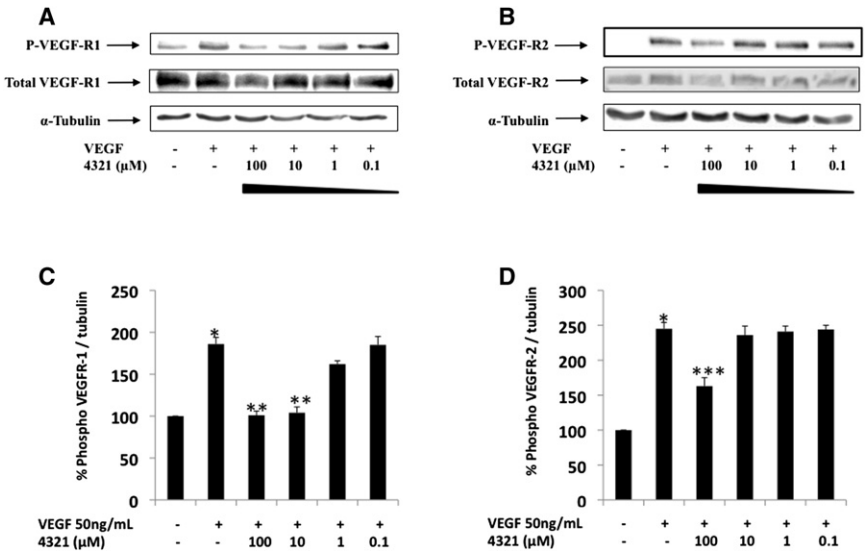

Figure 5. Compound 4321 Inhibits VEGF-Induced Phosphorylation of Both VEGFR-1 and VEGFR-2

Starved HUVECs were incubated with compound **4321** at the indicated concentration over a period of 1 hr and then stimulated by $VEGF_{165}$ 50 ng/ml during 5 min, cells were lysed, and cellular extracts were submitted to specific antibodies. Western blots were performed with anti-phospho-VEGFR-1 (P-VEGFR-1) and anti-VEGFR-1 (A) and anti-phospho-VEGFR-2 (P-VEGFR-2) and anti-VEGFR-2 (B), and in both cases anti-α-tubulin was used as control (data result from three independent experiments). Relative optical density of the bands in arbitrary units is represented for P-VEGFR-1 (C) and P-VEGFR-2 (D) both reported to the α-tubulin control. All results are expressed as mean ± SD. Control without VEGF is considered as 100%. *$p < 0.0001$ versus the group without $VEGF_{165}$; **$p < 0.0001$ and ***$p < 0.001$ versus the group with $VEGF_{165}$.

Procedures). HUVE cells (HUVECs), a widely used model for angiogenesis, were chosen for this study. Compound **4321** clearly inhibited VEGFR-1 phosphorylation at concentrations between 1 and 100 μM (Figure 5A and corresponding quantization in Figure 5C), whereas VEGFR-2 phosphorylation was partially inhibited only at 100 μM (Figures 5B and 5D). Thus, compound **4321** seems to decrease the phosphorylation of VEGFR-1 more efficiently than that of VEGFR-2.

Compound 4321 Inhibits the VEGF-Induced Formation of Tubule-like Structures in HUVECs

It has been shown that the induction of branching morphogenesis in HUVECs is dependent on VEGFRs. In a 3D Matrigel medium, mimicking the basal membrane, HUVECs branch to form tubule-like structures. This process mimics the endothelial tubulogenesis that occurs during the formation of new vessels. Once HUVECs were seeded on Matrigel, VEGF stimulation (50 ng/ml) induced a capillary tube network composed of cells that migrated and extended to join themselves (Figure 6A, VEGF alone). The negative control without VEGF (Figure 6A, No VEGF) displayed no structured capillary tube drafts. The treatment of HUVECs with molecule **4321** clearly inhibited the $VEGF_{165}$-induced endothelial cell tubulogenesis. Indeed, this molecule decreased the number of branching junctions formed by HUVECs on Matrigel in a dose-dependent manner (from 1 to 100 μM; quantization in Figure 6B), with no capillary tube formation; as for the negative control, when compound **4321** was used at concentrations of 100, 33, and 10 μM. Interestingly, in tests at a concentration of 10 μM, this molecule displayed no toxicity in WST-1 colorimetric tests on HUVECs.

These data confirm that **4321** compound preferentially targeted the VEGR-1 receptor. Moreover, the branching morphogenesis of HUVECs has been shown to be due to both migration and cell differentiation. Cell migration is a complex phenomenon that requires cytoskeleton-regulated cell motility and cell adhesion. Lauffenburger and Horwitz (1996) and Kanno et al. (2000) have shown that VEGFR-1 regulates cell migration through the modulation of actin reorganization. We, therefore, investigated the effect of compound **4321** on actin and tubulin organization. We chose to use a dose of only 10 μM for compound **4321**. At this concentration, this compound inhibited the phosphorylation of VEGFR-1, but not that of VEGFR-2 (Figure 5), and tube formation by HUVECs (Figure 6). Immunofluorescence experiments were then carried out with anti-actin and anti-tubulin antibodies (Figure S4). The stimulation of cells with 50 ng/ml VEGF elicited the reorganization of both the actin and tubulin networks. This phenomenon was clearly inhibited by 10 μM **4321**. Indeed, compound **4321** induced an effect similar to that induced by a specific and previously reported anti-VEGFR-1 antibody (Kanno et al., 2000). These results support the hypothesis that compound **4321** targets VEGFR-1.

SIGNIFICANCE

Common characteristics of protein-protein interfaces that have been inhibited by a small molecule were the presence of either a relatively deep binding groove or of several small subpockets (Fuller et al., 2009). In our case, although the VEGF-VEGFR-1 interface is very flat, we could find three subpockets. We performed a conformational search and docking computations over a large area that extended outside the direct protein-protein interface. The success of the in silico screening on this flat surface could be due to both the presence of small cavities and the overall rigidity of the region. Furthermore, it would be interesting to explore if the size and physicochemical nature of the compounds could play a role in addressing flat interfaces.

Overall, we have identified 20 compounds disrupting one of the flattest known therapeutically important protein-protein interfaces (hit rate, 9.7%). To the best of our knowledge, our best inhibitor is the first drug-like molecule discovered by structure-based screening to inhibit specifically the formation of the VEGFR-1-VEGF complex. This inhibitor is easy to synthesize, is smaller (molecular mass, 304 kDa) than many previously reported PPI inhibitors (Sperandio et al., 2010b), and has a reasonable ligand efficiency

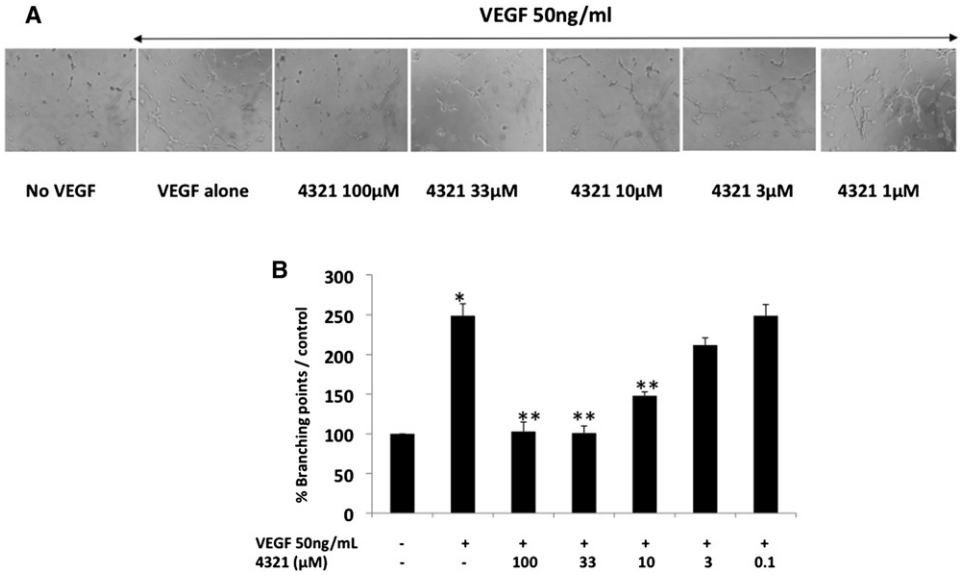

Figure 6. Effect of Compound 4321 on Tubule Formation Network

(A) HUVECs were seeded on Matrigel with or without 50 ng/ml of $VEGF_{165}$ in the presence or the absence of compound **4321** at the indicated concentrations. Tube-like structures were visualized 4 hr later.

(B) Tube-like structures formation was quantified by the number of branching points. The control without $VEGF_{165}$ is considered as 100%, and results are expressed as the mean ± SD. *$p < 0.0001$ versus the group without $VEGF_{165}$; **$p < 0.0001$ versus the group with $VEGF_{165}$.

See Figure S4.

(0.32 kcal mol^{-1} per nonhydrogen atom). Many recent publications have described the role of VEGFR-1 in cancers such as breast cancer, acute myeloid leukemias, and acute lymphoblastic leukemia (Dales et al., 2003; Fragoso et al., 2006; Hiratsuka et al., 2001, 2002; Kracmarova et al., 2008; Luttun et al., 2004; Stefanik et al., 2001). Our best molecule, 4321, prevented VEGFR-1 signaling pathway and is more specific for VEGFR-1 than VEGFR-2. Thus, molecule 4321 constitutes a potent pharmacological probe for studies of cancer and other angiogenesis-driven disorders, and our results support the idea of developing PPI inhibitors even for flat interfaces.

EXPERIMENTAL PROCEDURES

The CERMN Compound Collection

The CERMN-Normandy Drug Study and Research Center (http://www.cermn.unicaen.fr/) collection is part of the French compound library initiative and contains over 8,000 original molecules that have been synthesized for drug discovery projects (Hibert, 2009).

Target and Compound Preparation and In Silico Screening Protocol

The structure of the VEGFR-1 protein target was obtained from the X-ray structure of the VEGF-VEFGR-1 D2 complex (PDB ID: 1FLT, resolution 1.70 A). For VEGFR-1 the protonation states of residues were assigned at pH 7.0, after computations with the Protein Continuum Electrostatic server (Miteva et al., 2005b). Binding pocket predictions were carried out with two probe-mapping methods: LigBuilder (Wang et al., 2000) and Surflex (Jain, 2003). All 8,000 molecules of the CERNM collection were docked. We generated a single 3D conformer for each molecule with our in-house program DG-AMMOS (Lagorce et al., 2009). The top 2,500 docked poses, with the best Surflex scores (between 7.67 and 4.60), were analyzed with PyMOL (DeLano, San Carlos, CA), and 350 molecules were selected. Additional docking experiments of the best compound, molecule **4321**, were performed with AutoDock4 (Morris et al., 2009) with some side chains in the binding area allowed to be flexible during the docking runs (see Supplemental Experimental Procedures for detailed explanations).

HUVEC Culture

HUVECs were cultured in EGM-2 at 37°C, in a humidified atmosphere containing 5% CO_2 in air, and the medium was changed every 2 days. HUVECs were used for experiments from the second to the fifth passage.

In Vitro VEGFR-1 Chemiluminescent Assay

The assay was performed as previously described (Goncalves et al., 2008). Briefly, a fixed amount of biotinylated human $VEGF_{165}$ (131 pM) was incubated with the screened compounds in a 96-well microplate coated with a human VEGFR-1 ECD/Fc chimera or a VEGFR-1 D1–D3 domains/Fc chimera. The residual $btVEGF_{165}$ present after washing was detected by chemiluminescent with horseradish peroxidase-conjugated streptavidin.

Western Blot Analysis

The western blot experiments were performed as previously described (Goncalves et al., 2008), but with some modifications. Confluent HUVECs in 6-well plates were starved by incubation overnight in EBM-2 without supplements. HUVECs were incubated with compounds for 1 hr, at the indicated concentrations, and were then stimulated with 50 ng/ml (131 nM) $VEGF_{165}$ for 5 min. HUVECs were lysed in 1% NP40 plus 1% Bridj 96 lysis buffer. The lysate was subjected to SDS-PAGE in an 8% polyacrylamide gel, and the resulting bands were transferred onto nitrocellulose membranes. The membranes were incubated with the indicated antibodies at a dilution of 1:1,000, with the exception of the anti-tubulin antibody, which was used at a dilution of 1:20,000. Antibody binding was detected by enhanced chemiluminescence with a CCD camera (Fisher Bioblock Scientific, Illkirch, France), and densitometry analysis was performed with Chemicapt 3000 software (Fisher Bioblock Scientific). The results are expressed assuming a value of 100% for the untreated wells.

Formation of Tubule-like Structures

We added 75 µl of Matrigel containing only low levels of growth factors to a 96-well microplate and allowed polymerization to occur at 37°C for 30 min. Confluent HUVECs were cultured overnight in EBM-2 without

supplements or FBS, and the cells (2×10^4) were then used to seed wells containing EBM-2 alone or supplemented with 50 ng/ml (1.3 nM) $VEGF_{165}$, in the presence or absence of various compounds at the concentrations indicated. Four hours later, the endothelial cell-derived tube-like structures were visualized under an inverted microscope and photographed at a magnification of ×20. The formation of tube-like structures was quantified by calculating the number of branching points with ImageJ software. Results are expressed assuming a value of 100% for untreated cells.

Expression, Purification, and Folding of VEGFR-1 D2

The VEGFR-1 D2 domain (residues 133–225) was cloned into the pet22 expression vector (Novagen) and transformed in *E. coli* Rosetta-gami (DE3) pLysS bacterial strain (Novagen). Cultures were grown at 37°C in LB supplemented with 150 μg/l ampicillin. When the cell density reached an OD of 0.4 at 600 nm, protein expression was induced by the addition of 0.4 mM isopropyl β-D-1-thiogalactopyranoside. VEGFR-1 D2 was expressed as insoluble protein. After 4 hr, cells were harvested by centrifugation and resuspended in Tris/HEPES buffer (50 mM/50 mM [pH 8.1]) containing 1% (W/V) Triton X-100. Cells were lysed by ultrasonic disruption. Inclusion bodies were isolated by centrifugation at 9,500 × *g* during 20 min at 4°C. The pellet was submitted to this treatment (resuspension, sonication, centrifugation) three additional times. Dried pellet (0.625 g) was suspended by sonication in 1 ml Tris/HEPES 50 mM (pH 8.1), DTT 20 mM, then solubilized in 30 ml urea 8 M HEPES/NaOH 25 mM (pH 6.8) (solution A [Sol. A]). Solubilized VEGFR-1 D2 was purified by cation-exchange chromatography on a source 15 S column (Amersham) previously equilibrated with Sol. A, and eluted by Sol. A plus NaCl 1 M. Unfolded D2 purified in urea reached 190 mg for 1 liter of *E. coli* culture.

Refolding was performed as follows. Solubilized VEGFR-1 D2 (0.5 mg/ml) was dialyzed overnight against 20 vol HEPES 25 mM (pH 6.8) at 4°C. Dialysis was repeated once in the same conditions. A total of 600 mM (NH4)2SO4 was then added to precipitate misfolded protein. Insoluble material was isolated by centrifugation at 9,500 × *g* during 15 min at 4°C and recycled by solubilization in Sol. A without further reduction. It was refolded following the same protocol. This was repeated several times leading to a final refolding rate of 70%. Soluble refolding products were further purified on a Phenyl Sepharose column (Amersham) equilibrated with HEPES/NaOH 25 mM (pH 6.8) plus 600 mM (NH4)2SO4 and eluted by a linear gradient of HEPES/NaOH 25 mM (pH 6.8). Typical results are 70 mg of folded and purified VEGFR-1 D2 for 1 liter of initial cell culture. The protein was lyophilized for long-range storage.

NMR Experiments

All NMR spectra were recorded at 293 K on a 600 MHz Bruker Avance spectrometer equipped with a 5 mm triple resonance inverse probe and an xyz gradient unit. A 1D ^{1}H-NMR reference spectrum was recorded for compound **4321** in the presence and the absence of the protein VEGFR-1 D2. The small molecule was prepared at a concentration of 500 μM, and the protein VEGFR-1 D2 was added at the concentration of 25 μM in H_2O/D20 (90/10). DMSO-d6 (5%) was added to solubilize the compound in H_2O. Water suppression was achieved by using excitation sculpting with gradient sequence (Hwang and Shaka, 1995). WaterLOGSY NMR experiments (Dalvit et al., 2001) used a 5 ms selective Gaussian 180° pulse at the water signal frequency and a 1.1 s NOE mixing time. The spectra were recorded with a spectral width of 6009 Hz, a 3 s relaxation delay, 128 scans for the 1D reference spectra, and 1 or 3 k scans for the WaterLOGSY spectra.

Statistical Analysis

For IC_{50} determination, each experiment was performed three times in triplicate. The data are expressed as mean of the three experiments and the corresponding SD. For biological experiments the statistically significant differences between the groups were determined via a two-way ANOVA followed by the Student's t test, in GraphPad Prism 3. Values of $p < 0.05$ were considered significant.

SUPPLEMENTAL INFORMATION

Supplemental Information includes four figures, two tables, and Supplemental Experimental Procedures and can be found with this article online at doi:10.1016/j.chembiol.2011.10.016.

ACKNOWLEDGMENTS

We would like to thank Paris Descartes University, Paris Diderot University, INSERM, and CNRS for support. We thank Dr. O. Taboureau for running our compounds through his hERG ion channel simulation model. We thank the national agency ANR (project SALSA) for financial support (grant number: ANR-2010-BLAN-1533) and the Perpignan University for BQR support. The authors have no competing financial interests.

Received: February 11, 2011
Revised: September 16, 2011
Accepted: October 24, 2011
Published: December 22, 2011

REFERENCES

Arkin, M.R., and Whitty, A. (2009). The road less traveled: modulating signal transduction enzymes by inhibiting their protein-protein interactions. Curr. Opin. Chem. Biol. *13*, 284–290.

Barleon, B., Totzke, F., Herzog, C., Blanke, S., Kremmer, E., Siemeister, G., Marmé, D., and Martiny-Baron, G. (1997). Mapping of the sites for ligand binding and receptor dimerization at the extracellular domain of the vascular endothelial growth factor receptor FLT-1. J. Biol. Chem. *272*, 10382–10388.

Cavasotto, C.N., Kovacs, J.A., and Abagyan, R.A. (2005). Representing receptor flexibility in ligand docking through relevant normal modes. J. Am. Chem. Soc. *127*, 9632–9640.

Chen, A., and Shapiro, M. (2000). NOE pumping. 2. A high-throughput method to determine compounds with binding affinity to macromolecules by NMR. J. Am. Chem. Soc. *122*, 414–415.

Dales, J.P., Garcia, S., Bonnier, P., Duffaud, F., Carpentier, S., Djemli, A., Ramuz, O., Andrac, L., Lavaut, M., Allasia, C., and Charpin, C. (2003). [Prognostic significance of VEGF receptors, VEGFR-1 (Flt-1) and VEGFR-2 (KDR/Flk-1) in breast carcinoma]. Ann. Pathol. *23*, 297–305.

Dalvit, C., Fogliatto, G., Stewart, A., Veronesi, M., and Stockman, B. (2001). WaterLOGSY as a method for primary NMR screening: practical aspects and range of applicability. J. Biomol. NMR *21*, 349–359.

D'Andrea, L.D., Iaccarino, G., Fattorusso, R., Sorriento, D., Carannante, C., Capasso, D., Trimarco, B., and Pedone, C. (2005). Targeting angiogenesis: structural characterization and biological properties of a de novo engineered VEGF mimicking peptide. Proc. Natl. Acad. Sci. USA *102*, 14215–14220.

Ferrara, N., and Kerbel, R.S. (2005). Angiogenesis as a therapeutic target. Nature *438*, 967–974.

Fragoso, R., Pereira, T., Wu, Y., Zhu, Z., Cabeçadas, J., and Dias, S. (2006). VEGFR-1 (FLT-1) activation modulates acute lymphoblastic leukemia localization and survival within the bone marrow, determining the onset of extramedullary disease. Blood *107*, 1608–1616.

Fry, D.C. (2008). Drug-like inhibitors of protein-protein interactions: a structural examination of effective protein mimicry. Curr. Protein Pept. Sci. *9*, 240–247.

Fuh, G., Wu, P., Liang, W.C., Ultsch, M., Lee, C.V., Moffat, B., and Wiesmann, C. (2006). Structure-function studies of two synthetic anti-vascular endothelial growth factor Fabs and comparison with the Avastin Fab. J. Biol. Chem. *281*, 6625–6631.

Fuller, J.C., Burgoyne, N.J., and Jackson, R.M. (2009). Predicting druggable binding sites at the protein-protein interface. Drug Discov. Today *14*, 155–161.

Garzón, J.I., Kovacs, J., Abagyan, R., and Chacón, P. (2007). DFprot: a webtool for predicting local chain deformability. Bioinformatics *23*, 901–902.

Gautier, B., Goncalves, V., Diana, D., Di Stasi, R., Teillet, F., Lenoir, C., Huguenot, F., Garbay, C., Fattorusso, R., D'Andrea, L.D., et al. (2010). Biochemical and structural analysis of the binding determinants of a vascular endothelial growth factor receptor peptidic antagonist. J. Med. Chem. *53*, 4428–4440.

Goncalves, V., Gautier, B., Coric, P., Bouaziz, S., Lenoir, C., Garbay, C., Vidal, M., and Inguimbert, N. (2007a). Rational design, structure, and biological evaluation of cyclic peptides mimicking the vascular endothelial growth factor. J. Med. Chem. *50*, 5135–5146.

Goncalves, V., Gautier, B., Garbay, C., Vidal, M., and Inguimbert, N. (2007b). Development of a chemiluminescent screening assay for detection of vascular endothelial growth factor receptor 1 ligands. Anal. Biochem. *366*, 108–110.

Goncalves, V., Gautier, B., Garbay, C., Vidal, M., and Inguimbert, N. (2008). Structure-based design of a bicyclic peptide antagonist of the vascular endothelial growth factor receptors. J. Pept. Sci. *14*, 767–772.

Grothey, A., and Galanis, E. (2009). Targeting angiogenesis: progress with anti-VEGF treatment with large molecules. Nat. Rev. Clin. Oncol. *6*, 507–518.

Hanahan, D., and Weinberg, R.A. (2000). The hallmarks of cancer. Cell *100*, 57–70.

Hibert, M.F. (2009). French/European academic compound library initiative. Drug Discov. Today *14*, 723–725.

Hicklin, D.J., and Ellis, L.M. (2005). Role of the vascular endothelial growth factor pathway in tumor growth and angiogenesis. J. Clin. Oncol. *23*, 1011–1027.

Higueruelo, A.P., Schreyer, A., Bickerton, G.R., Pitt, W.R., Groom, C.R., and Blundell, T.L. (2009). Atomic interactions and profile of small molecules disrupting protein-protein interfaces: the TIMBAL database. Chem. Biol. Drug Des. *74*, 457–467.

Hiratsuka, S., Maru, Y., Okada, A., Seiki, M., Noda, T., and Shibuya, M. (2001). Involvement of Flt-1 tyrosine kinase (vascular endothelial growth factor receptor-1) in pathological angiogenesis. Cancer Res. *61*, 1207–1213.

Hiratsuka, S., Nakamura, K., Iwai, S., Murakami, M., Itoh, T., Kijima, H., Shipley, J.M., Senior, R.M., and Shibuya, M. (2002). MMP9 induction by vascular endothelial growth factor receptor-1 is involved in lung-specific metastasis. Cancer Cell *2*, 289–300.

Holmes, K., Roberts, O.L., Thomas, A.M., and Cross, M.J. (2007). Vascular endothelial growth factor receptor-2: structure, function, intracellular signalling and therapeutic inhibition. Cell. Signal. *19*, 2003–2012.

Hwang, T.-L., and Shaka, A.J. (1995). Water suppression that works. Excitation sculpting using arbitrary waveforms and pulsed field gradients. J. Magn. Reson. A *112*, 275–279.

Ivy, S.P., Wick, J.Y., and Kaufman, B.M. (2009). An overview of small-molecule inhibitors of VEGFR signaling. Nat. Rev. Clin. Oncol. *6*, 569–579.

Jain, A.N. (2003). Surflex: fully automatic flexible molecular docking using a molecular similarity-based search engine. J. Med. Chem. *46*, 499–511.

Jänne, P.A., Gray, N., and Settleman, J. (2009). Factors underlying sensitivity of cancers to small-molecule kinase inhibitors. Nat. Rev. Drug Discov. *8*, 709–723.

Jia, H., Jezequel, S., Löhr, M., Shaikh, S., Davis, D., Soker, S., Selwood, D., and Zachary, I. (2001). Peptides encoded by exon 6 of VEGF inhibit endothelial cell biological responses and angiogenesis induced by VEGF. Biochem. Biophys. Res. Commun. *283*, 164–173.

Kanno, S., Oda, N., Abe, M., Terai, Y., Ito, M., Shitara, K., Tabayashi, K., Shibuya, M., and Sato, Y. (2000). Roles of two VEGF receptors, Flt-1 and KDR, in the signal transduction of VEGF effects in human vascular endothelial cells. Oncogene *19*, 2138–2146.

Keyt, B.A., Nguyen, H.V., Berleau, L.T., Duarte, C.M., Park, J., Chen, H., and Ferrara, N. (1996). Identification of vascular endothelial growth factor determinants for binding KDR and FLT-1 receptors. Generation of receptor-selective VEGF variants by site-directed mutagenesis. J. Biol. Chem. *271*, 5638–5646.

Kracmarova, A., Cermak, J., Brdicka, R., and Bruchova, H. (2008). High expression of ERCC1, FLT1, NME4 and PCNA associated with poor prognosis and advanced stages in myelodysplastic syndrome. Leuk. Lymphoma *49*, 1297–1305.

Lagorce, D., Sperandio, O., Galons, H., Miteva, M.A., and Villoutreix, B.O. (2008). FAF-Drugs2: free ADME/tox filtering tool to assist drug discovery and chemical biology projects. BMC Bioinformatics *9*, 396.

Lagorce, D., Pencheva, T., Villoutreix, B.O., and Miteva, M.A. (2009). DG-AMMOS: a new tool to generate 3d conformation of small molecules using distance geometry and automated molecular mechanics optimization for in silico screening. BMC Chem. Biol. *9*, 6.

Lagorce, D., Maupetit, J., Baell, J., Sperandio, O., Tufféry, P., Miteva, M.A., Galons, H., and Villoutreix, B.O. (2011). The FAF-Drugs2 server: a multistep engine to prepare electronic chemical compound collections. Bioinformatics *27*, 2018–2020.

Lauffenburger, D.A., and Horwitz, A.F. (1996). Cell migration: a physically integrated molecular process. Cell *84*, 359–369.

Li, B., Fuh, G., Meng, G., Xin, X., Gerritsen, M.E., Cunningham, B., and de Vos, A.M. (2000). Receptor-selective variants of human vascular endothelial growth factor. Generation and characterization. J. Biol. Chem. *275*, 29823–29828.

Luttun, A., Autiero, M., Tjwa, M., and Carmeliet, P. (2004). Genetic dissection of tumor angiogenesis: are PlGF and VEGFR-1 novel anti-cancer targets? Biochim. Biophys. Acta *1654*, 79–94.

Mayer, M., and Meyer, B. (1999). Characterization of ligand binding by saturation transfer difference NMR spectroscopy. Angew. Chem. Int. Ed. Engl. *38*, 1784–1788.

Meyer, B., Weimar, T., and Peters, T. (1997). Screening mixtures for biological activity by NMR. Eur. J. Biochem. *246*, 705–709.

Miteva, M.A., Lee, W.H., Montes, M.O., and Villoutreix, B.O. (2005a). Fast structure-based virtual ligand screening combining FRED, DOCK, and Surflex. J. Med. Chem. *48*, 6012–6022.

Miteva, M.A., Tufféry, P., and Villoutreix, B.O. (2005b). PCE: web tools to compute protein continuum electrostatics. Nucleic Acids Res. *33* (Web Server issue), W372–W375.

Morris, G.M., Huey, R., Lindstrom, W., Sanner, M.F., Belew, R.K., Goodsell, D.S., and Olson, A.J. (2009). AutoDock4 and AutoDockTools4: automated docking with selective receptor flexibility. J. Comput. Chem. *30*, 2785–2791.

Muller, Y.A., Li, B., Christinger, H.W., Wells, J.A., Cunningham, B.C., and de Vos, A.M. (1997). Vascular endothelial growth factor: crystal structure and functional mapping of the kinase domain receptor binding site. Proc. Natl. Acad. Sci. USA *94*, 7192–7197.

Olsson, A.K., Dimberg, A., Kreuger, J., and Claesson-Welsh, L. (2006). VEGF receptor signalling - in control of vascular function. Nat. Rev. Mol. Cell Biol. *7*, 359–371.

Pan, B., Li, B., Russell, S.J., Tom, J.Y., Cochran, A.G., and Fairbrother, W.J. (2002). Solution structure of a phage-derived peptide antagonist in complex with vascular endothelial growth factor. J. Mol. Biol. *316*, 769–787.

Reynolds, C., Damerell, D., and Jones, S. (2009). ProtorP: a protein-protein interaction analysis server. Bioinformatics *25*, 413–414.

Ruch, C., Skiniotis, G., Steinmetz, M.O., Walz, T., and Ballmer-Hofer, K. (2007). Structure of a VEGF-VEGF receptor complex determined by electron microscopy. Nat. Struct. Mol. Biol. *14*, 249–250.

Shibuya, M., Yamaguchi, S., Yamane, A., Ikeda, T., Tojo, A., Matsushime, H., and Sato, M. (1990). Nucleotide sequence and expression of a novel human receptor-type tyrosine kinase gene (flt) closely related to the fms family. Oncogene *5*, 519–524.

Sperandio, O., Miteva, M.A., Delfaud, F., and Villoutreix, B.O. (2006). Receptor-based computational screening of compound databases: the main docking-scoring engines. Curr. Protein Pept. Sci. *7*, 369–393.

Sperandio, O., Mouawad, L., Pinto, E., Villoutreix, B.O., Perahia, D., and Miteva, M.A. (2010a). How to choose relevant multiple receptor conformations for virtual screening: a test case of Cdk2 and normal mode analysis. Eur. Biophys. J. *39*, 1365–1372.

Sperandio, O., Reynès, C.H., Camproux, A.C., and Villoutreix, B.O. (2010b). Rationalizing the chemical space of protein-protein interaction inhibitors. Drug Discov. Today *15*, 220–229.

Starovasnik, M.A., Christinger, H.W., Wiesmann, C., Champe, M.A., de Vos, A.M., and Skelton, N.J. (1999). Solution structure of the VEGF-binding domain of Flt-1: comparison of its free and bound states. J. Mol. Biol. *293*, 531–544.

Stefanik, D.F., Fellows, W.K., Rizkalla, L.R., Rizkalla, W.M., Stefanik, P.P., Deleo, A.B., and Welch, W.C. (2001). Monoclonal antibodies to vascular endothelial growth factor (VEGF) and the VEGF receptor, FLT-1, inhibit the growth of C6 glioma in a mouse xenograft. J. Neurooncol. *55*, 91–100.

Stumpf, M.P., Thorne, T., de Silva, E., Stewart, R., An, H.J., Lappe, M., and Wiuf, C. (2008). Estimating the size of the human interactome. Proc. Natl. Acad. Sci. USA *105*, 6959–6964.

 ©2011 Elsevier Ltd All rights reserved

Terman, B.I., Carrion, M.E., Kovacs, E., Rasmussen, B.A., Eddy, R.L., and Shows, T.B. (1991). Identification of a new endothelial cell growth factor receptor tyrosine kinase. Oncogene *6*, 1677–1683.

Ueda, Y., Yamagishi, T., Ikeya, H., Hirayama, N., Itokawa, T., Aozuka, Y., Samata, K., Nakaike, S., Tanaka, M., Ono, M., and Saiki, I. (2004a). VGA1155, a novel binding antagonist of VEGF, inhibits angiogenesis in vitro and in vivo. Anticancer Res. *24* (5A), 3009–3017.

Ueda, Y., Yamagishi, T., Samata, K., Ikeya, H., Hirayama, N., Okazaki, T., Nishihara, S., Arai, K., Yamaguchi, S., Shibuya, M., et al. (2004b). A novel low molecular weight VEGF receptor-binding antagonist, VGA1102, inhibits the function of VEGF and in vivo tumor growth. Cancer Chemother. Pharmacol. *54*, 16–24.

Villoutreix, B.O., Bastard, K., Sperandio, O., Fahraeus, R., Poyet, J.L., Calvo, F., Déprez, B., and Miteva, M.A. (2008). In silico-in vitro screening of protein-protein interactions: towards the next generation of therapeutics. Curr. Pharm. Biotechnol. *9*, 103–122.

Wang, R., Gao, Y., and Lai, L. (2000). LigBuilder: a multi-purpose program for structure-based drug design. J. Mol. Model. *6*, 498–516.

Wells, J.A., and McClendon, C.L. (2007). Reaching for high-hanging fruit in drug discovery at protein-protein interfaces. Nature *450*, 1001–1009.

Wiesmann, C., Fuh, G., Christinger, H.W., Eigenbrot, C., Wells, J.A., and de Vos, A.M. (1997). Crystal structure at 1.7 A resolution of VEGF in complex with domain 2 of the Flt-1 receptor. Cell *91*, 695–704.

Ziche, M., Maglione, D., Ribatti, D., Morbidelli, L., Lago, C.T., Battisti, M., Paoletti, I., Barra, A., Tucci, M., Parise, G., et al. (1997). Placenta growth factor-1 is chemotactic, mitogenic, and angiogenic. Lab. Invest. *76*, 517–531.

Zilberberg, L., Shinkaruk, S., Lequin, O., Rousseau, B., Hagedorn, M., Costa, F., Caronzolo, D., Balke, M., Canron, X., Convert, O., et al. (2003). Structure and inhibitory effects on angiogenesis and tumor development of a new vascular endothelial growth inhibitor. J. Biol. Chem. *278*, 35564–35573.